geoconvention
Virtual Event
September 13 - 15 2021

Diffraction Multifocusing Stacking With The Watershed Transform

C.Robert Pinnegar and C.Torr Haglund
Statcom Ltd.

Summary

Diffraction multifocusing stacking (DMFS) is a technique developed by Berkovitch et al. (2009) to identify and resolve diffractions in seismic data. Several industry papers have been published over the past ten years that present results of the technique, but, in general, these have provided few details of the implementation or workflow. This poster describes our implementation of DMFS and presents some results of applying it to exploration data. The method does enhance diffraction energy, but has trouble dealing with residual specular reflections, and therefore is currently limited to datasets for which *f-k* filtering can be used to remove reflections from the input data (viz. those that do not include strongly dipping reflectors).

Theory / Method / Workflow

DMFS is a modification of velocity analysis that differs from conventional velocity analysis in two important respects. The first is that common-midpoint (CMP) gathers are replaced with “circle gathers” that include all traces whose source and receiver positions lie within a user-defined radius of the bin position. (The radius restriction addresses the rapid amplitude decay with distance of diffracted wave energy.)

The second difference is that the zero-offset raypath to which input travel times are corrected is not assumed to be vertical, as with normal-moveout (NMO) correction. The raypath can have a nonzero tilt from the vertical (we call this tilt “dip”, by analogy with NMO), and an associated azimuth. The two-way zero-offset raypath then represents diffraction of energy straight back toward the incident direction from a laterally displaced diffractor, as in Figure 1. This type of moveout correction allows diffracted wave amplitudes to stack constructively at all nearby bin positions, not only at the bin that is directly above the diffractor.

Both of these modifications are designed to enhance diffraction energy, and to de-emphasize specular reflection energy, during the stacking process.

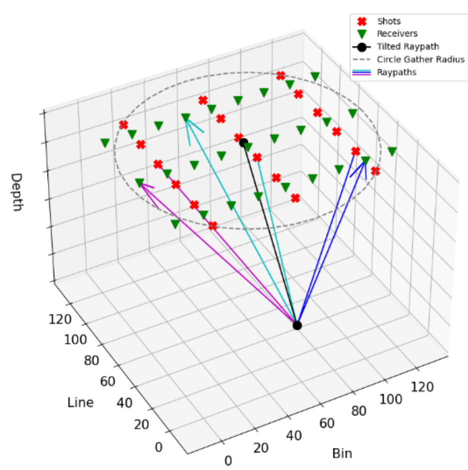

Figure 1: Circle gather, showing several shot-diffractor-receiver raypaths (coloured lines) and a tilted zero-offset raypath (black line).

Since no information about the locations of diffractors relative to any particular bin is available *a priori*, to detect diffractions we must perform moveout correction for many zero-offset raypaths at each bin, then search through the resulting stacked volume. This volume has five dimensions: the familiar line, bin, and time indices (ℓ, b, t), along with two new dimensions that represent the dip β and azimuth ϕ of each zero-offset raypath. In our implementation, the (β, ϕ) pairs are obtained from a geodesic grid that is generated by subdividing an icosahedron (Figure 2). The velocity field used to perform the moveout corrections is obtained from conventional velocity analysis, which we assume has already been performed.

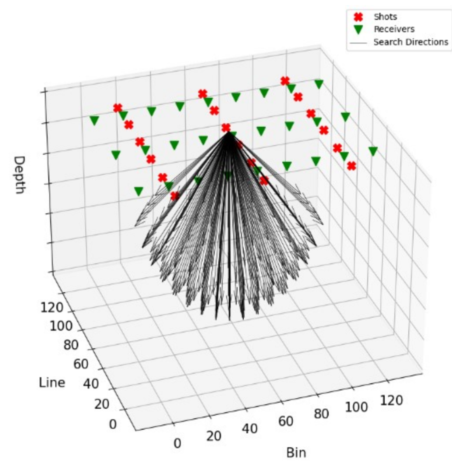

Figure 2: Suite of zero-offset raypaths (black quivers) for which DMFS must be performed at each bin to locate diffractors. These form a geodesic grid in dip/azimuth space; here azimuth is measured clockwise from the positive inline direction (the "Bin" axis).

Another way of looking at this is that, instead of returning a single stacked trace at each bin position, DMFS returns a whole ensemble of stacked traces at each bin, with each stacked trace corresponding to a different dip/azimuth pair.

It then remains to find ways of identifying diffractions in this five-dimensional stacked volume; muting all stacked amplitudes that do not represent diffraction energy; and then, at each bin position, collapsing the ensemble of stacked traces down to a single trace, to give 3-D output in (ℓ, b, t) space for interpretation and/or poststack migration. As might be expected, this is a complex multi-stage process that presents many challenges. One major complication is that individual diffractions often exhibit significant stacked amplitude across multiple adjacent geodesic grid positions in (β, ϕ) space. This causes a problem, because any particular diffraction should be included only once during the collapsing process at each bin, to avoid getting incorrect amplitudes in the output.

To this end, we calculate not only stacked amplitude at each pixel, but also semblance, giving a five-dimensional semblance volume to accompany the stacked volume. Semblance peaks that have significant volume extent and amplitude prominence, and which associate with large folds, often correspond to diffractions on the stacked data at the same co-ordinates. At each (l, b) bin, the (t, β, ϕ) positions of these semblance maxima then identify each diffraction uniquely with a specific (β, ϕ) direction. This tells us which stacked traces to retain during the collapsing process. Time windows can also be applied to each selected stacked trace, by using the time extents of its corresponding semblance peak around the *t* of maximum semblance to estimate the diffraction start and end times. These time extents, and the overall volume extent of each peak, can be obtained from the watershed transform (e.g. Kornilov and Safonov, 2018), a multidimensional mapping that groups together pixels that associate with the same local peak. Our method uses the multidimensional watershed transform from the Python Scikit-Image package.

Figure 3 shows cross-sections through a semblance volume that was generated by applying DMFS to a test dataset. We have found that, at any particular bin position, the dip/azimuth co-ordinates of large semblance peaks typically "point" in the directions of the apices of diffractions that can be seen on the conventional stack. The zero-offset travel times associated with these semblance peaks also typically agree with what would be expected from the vantage point of that bin position in the RMS approximation. Most tellingly, advancing through the line and bin directions (while holding time constant) leads to changes in the dip/azimuth co-ordinates of the semblance peaks that are consistent with perspective changes. This supports the idea that these semblance peaks are associated with real diffractors in the subsurface.

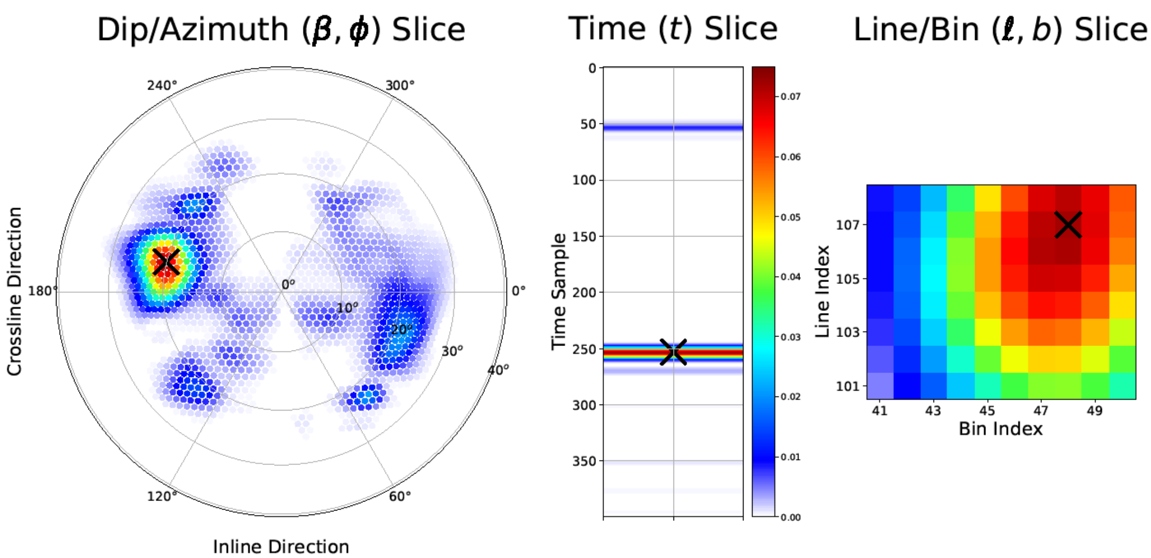

Figure 3: 5-D semblance volume, showing diffraction peaks. The subplots display three sections of the volume through the same point in $(\ell, b, t, \beta, \phi)$ space. Its co-ordinates are given by the X in all three subplots.

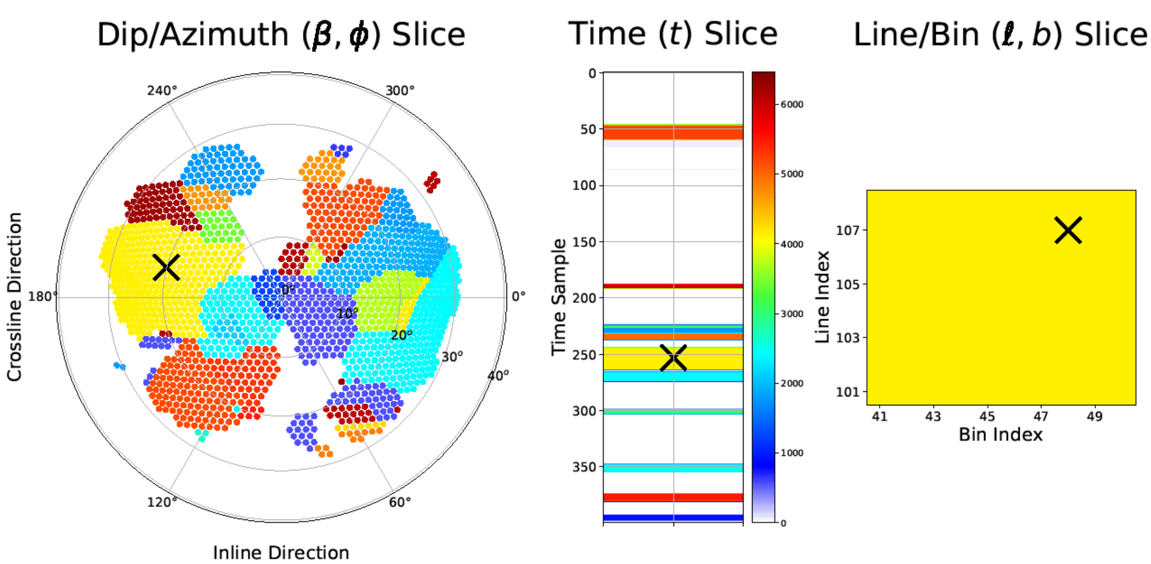

Figure 4: 5-D watershed transform of the semblance data from Figure 3, showing the spatial extent of each local maximum. The rightmost subplot has constant colour because, at the (t, β, ϕ) co-ordinates of the X, all points in (ℓ, b) space belong to the same local maximum.

Results, Observations, Conclusions

Ideally, we would like to be able to delineate the boundaries of semblance peaks using a five-dimensional watershed transform (e.g. Figure 4), the output of which would give information about how peaks connect laterally from line to line and bin to bin. However, computer memory limitations and run-time concerns restrict the spatial range of the five-dimensional transform. For our test data, only 8 lines by 10 bins could be managed. This area is not large enough to validate the technique.

The next-best approach is to identify diffractions by performing separate three-dimensional watershed transforms, in (t, β, ϕ) space, at each bin position. This approach often does produce well-defined diffraction hyperbolae on the collapsed stack; but the lack of lateral correlation can cause problems. The main difficulty is that the collapsing process necessarily requires criteria to determine which semblance peaks correspond to real diffractions that should be retained on the stack (for example, defining minimum thresholds for semblance amplitude and stacking fold can help to exclude spurious peaks). When the three-dimensional watershed transform is used, this assessment must be carried out separately at each bin position. Sometimes, the selection algorithm will retain a semblance peak at some bin positions but exclude it at others. This leads to gaps in the output hyperbolae, with consequent problems for poststack migration.

As might be expected for a new geophysical technique, DMFS has other implementation problems. The most significant is that destructive interference of reflection energy during stacking does not remove specular reflections as efficiently as might be hoped. To obtain useful results for our test dataset, we had to run the input data through an *f-k* filter to remove reflections before applying DMFS. Clearly, this approach would not be appropriate if the dataset had any strongly dipping reflectors. Figures 5 and 6 show one line of 3-D data after conventional velocity analysis and stacking; and the same line after *f-k* filtering followed by DMFS analysis. Performing DMFS without initial *f-k* filtering usually produces a result whose appearance lies somewhere between these two extremes.

Another problem is that, even after reflection energy has been removed, DMFS sometimes generates spurious semblance peaks. These tend to line up with the survey directions, leading to footprint artifacts in the collapsed output. The large folds of the circle gathers, and the multidimensional nature of the stacked data, make the source of these spurious peaks difficult to identify and address.

Novel/Additive Information

Previous DMFS publications (e.g. Berkovitch et al., 2012; Rauch-Davies et al., 2014), have mentioned semblance, but have not shown what semblance peaks that are due to diffractions look like in multidimensional space, or provided much discussion of the methodology involved in identifying peaks and connecting them with diffractions within the stacked volume. We have shown at least some details of both.

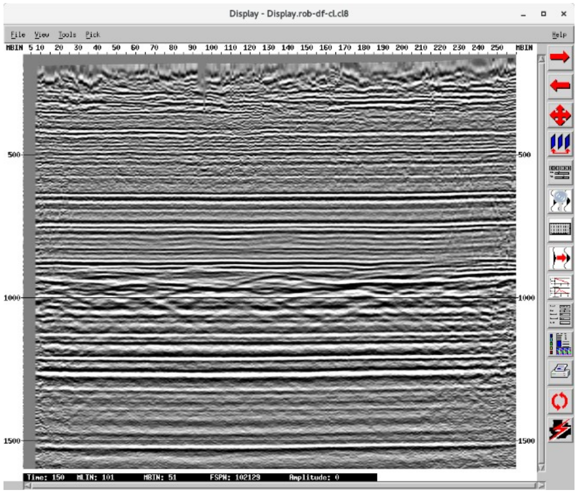

Figure 5: Line of conventional 3-D stack, unmigrated. Some diffraction hyperbolas are visible.

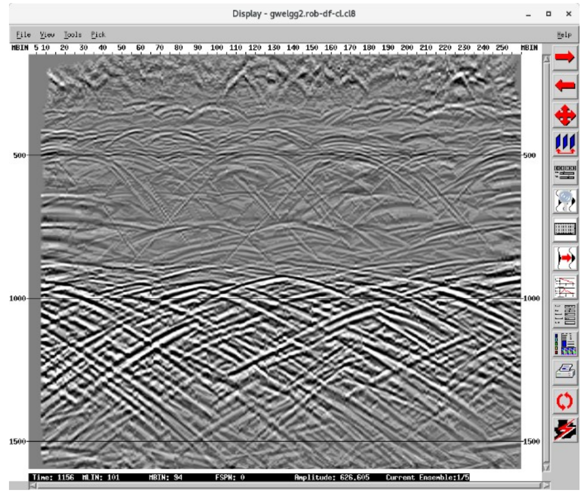

Figure 6: The same line after DMFS. Note that, unlike the case of Figure 5, the original input gathers were run through f-k filtering to remove reflections before processing.

Acknowledgements

The authors thank Alex Wright, Steve Bennett, Geoff Eikerman, Thomas Chew, Darrel Hemsing, and Jason Whitwell for their help during the various phases of this work.

This research was supported by a grant from the National Research Council of Canada Industrial Research Assistance Program (NRC IRAP).

References

Berkovitch, A., Belfer, I., Hassin, Y., and Landa, E., 2009, Diffraction imaging by multifocusing, Geophysics 74, WCA 75-81.

Berkovitch, A., Deev, K., Pelman, D., and Rauch-Davies, M., 2012, Multifocusing 3D diffraction imaging, 74th EAGE Conference & Exhibition, Copenhagen, Denmark.

Kornilov, A.S., Safonov, I.V., An overview of watershed algorithm implementations in open source libraries, Journal of Imaging 2018 (4), 123.

Rauch-Davies, M., Deev, K., Pelman, D., and Kachkachev-Shuifer, M., 2014, Diffraction imaging applied to pre-existing 3D seismic data to map fracture corridors in an unconventional play, First Break 32, 87-90.